APPENDIX A

TOWARDS THE SYNTHESIS OF HETEROMETALLIC MULTINUCLEAR

COMPLEXES AS MODELS OF [NIFE]-CARBON MONOXIDE

DEHYDROGENASE

Abstract

Synthetic models of [NiFe] carbon monoxide dehydrogenase (CODH) were targeted with the aim of isolating open heterobimetallic edge sites in [Fe_3Ni] clusters that mimic parts of both the [Fe_3NiS_4]-cubane and exo Fe site of the enzymatic active site. While a cationic [$Fe^{II}_3(\mu_3$-S)] cluster could be accessed, its application to higher nuclearity clusters proved challenging, and no nickel containing clusters could be isolated. A [$Fe^{III}_2Fe^{II}Ni^{II}(\mu_4$-O)] cluster could be isolated with the apical nickel center supported by both a chelating bis(oximate) ligand (**PRABOH₂**) and an acetate ligand. However, efforts to open a heterobimetallic edge site with electrophiles resulted in loss of both the nickel center and **PRABOH₂** ligand. While overall unsuccessful, this project provided insight into several design principles for the rational construction of heterometallic trinuclear complexes supported by the previously reported tris(alkoxide) hexa(pyridyl) ligand framework.

INTRODUCTION

The reduction of carbon dioxide and subsequent conversion into lower oxygen content products and liquid fuels is an area of active research due its relative abundance and identity as a greenhouse gas.[1] In biology, the selective two proton / two electron reduction of carbon dioxide (CO_2) to carbon monoxide (CO) can be reversibly mediated by the enzyme carbon monoxide dehydrogenase (CODH) at a heterobimetallic [Fe4Ni] cluster (Figure 1).[2] In a CO_2-coordinated solid-state structure obtained for the enzyme, the core of inorganic cofactor structurally resembles an [Fe4S4] cubane with one metal vertex replaced with a nickel center, which shows an elongated interaction with S4, resulting in an open cubane structure.[2b] Instead, S4 binds a fourth Fe center exo to the cubane. At this unique [NiFe] heterobimetallic edge site is where the reversible conversion of CO_2 and CO occurs through the mechanism proposed in Figure 1B.
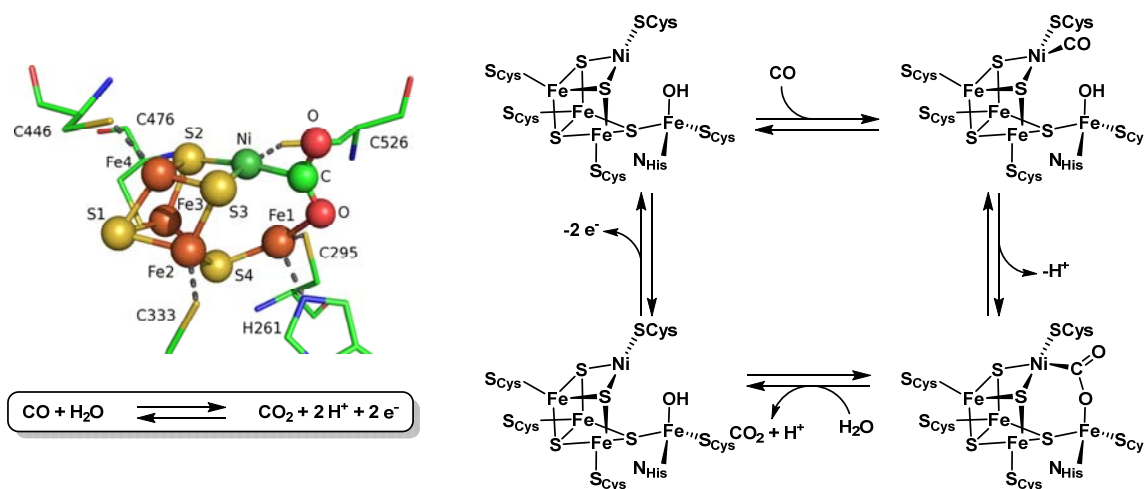
Figure 1. A) Active site structure of [NiFe]-CODH and B) proposed enzymatic catalytic cycle. Image credit for the pymol figure for [NiFe]-CODH goes to Dr. Davide Lionetti.

To better understand the enzymatic mechanism, many synthetic models of the [NiFe] CODH active site have been developed (Figure 2).[3] While a complete structural model of the active site have not been reported to date, likely attributable to the complexity and asymmetry of the target [Fe$_4$Ni] cluster, various aspects of the native cofactor, including heterometallic [NiFe] complexes,[3b] the [Fe$_3$Ni] cubane,[3a, 3c] and relevant fundamental chemical transformations at monometallic Ni complexes,[3d] the have been successfully incorporated in synthetic complexes. However, the coordination of CO$_2$ or hydroxide attack onto CO has not been demonstrated at [NiFe] complexes to date.
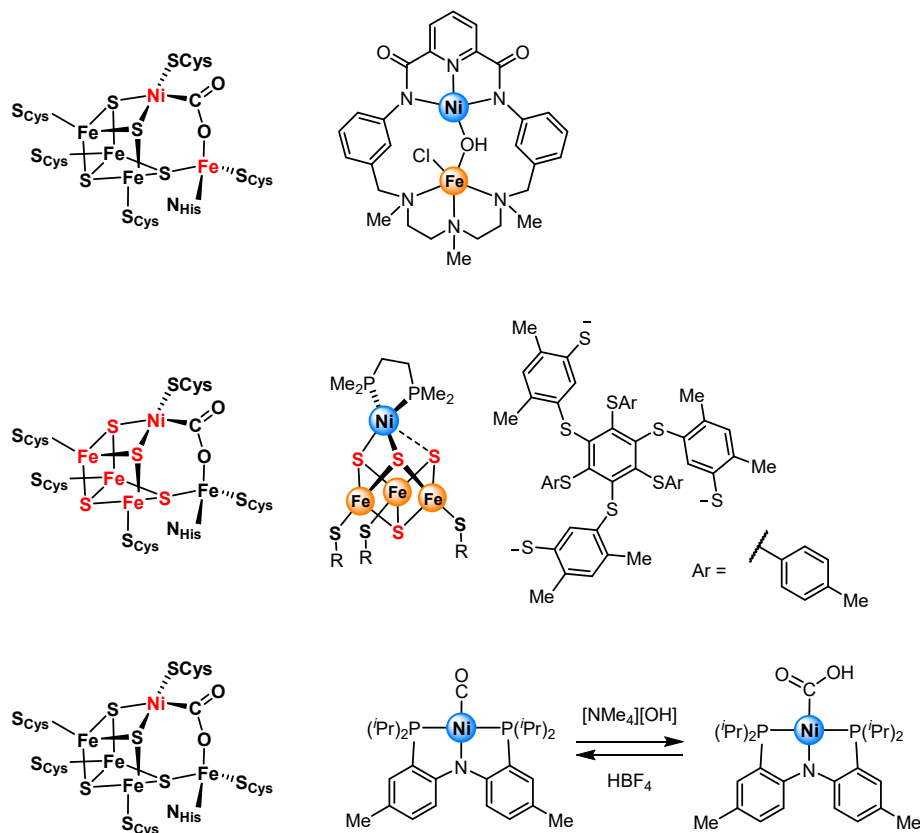
Figure 2. Select reported [NiFe] CODH model complexes and the modeled portions of the enzymatic active site.

Our group has previously reported the rational synthesis of numerous heterometallic multinuclear clusters supported by a tris(alkoxide) hexa(pyridyl) ligand framework (**LH₃**, Figure 3).[4] While these systems have provided insight into relationship between redox-active metals and the Lewis acidity of redox-inactive metals in [M₃M'(μ₄-O)(μ₂-OH)] (M = Mn, Fe) and Mn₃MO₄ cubanes, the extension of these clusters to small molecule activation has not been reported. Herein, we discuss the attempts to synthesize [Fe₃Ni(μ₄-X)]-type clusters with open edge sites capable of coordinating carbon dioxide to mimic the enzymatic active site of [NiFe] CODH (Figure 3). This strategy aims to model the [NiFe] heterobimetallic edge site as well as two additional Fe centers contained within the cubane moiety. Triiron tris(acetate) precursors support by **LH₃** have previously been reported in our group and will serve as an entry point into this chemistry. The triiron core is rigidly locked into a chair cyclohexane-like arrangement, which for the remainder of figures in this appendix will be abbreviated as a triangular arrangement of Fe centers as this core geometry remains invariant throughout the described chemistry (Figure 3).
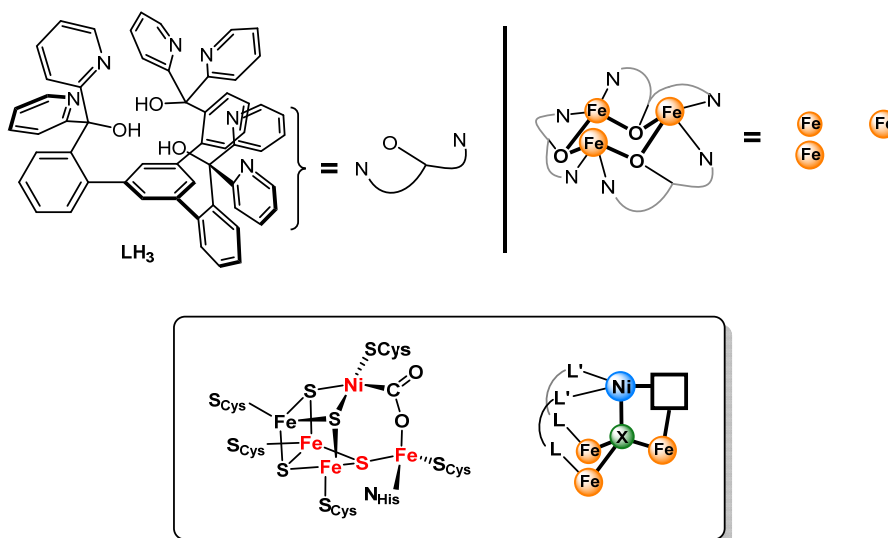
Figure 3. Targeted [Fe₃Ni(μ₄-X)] complexes as novel models of the [NiFe] CODH.

RESULTS AND DISCUSSION

Section A.1 Ligand Syntheses

Scheme 1. Syntheses of surveyed ligands
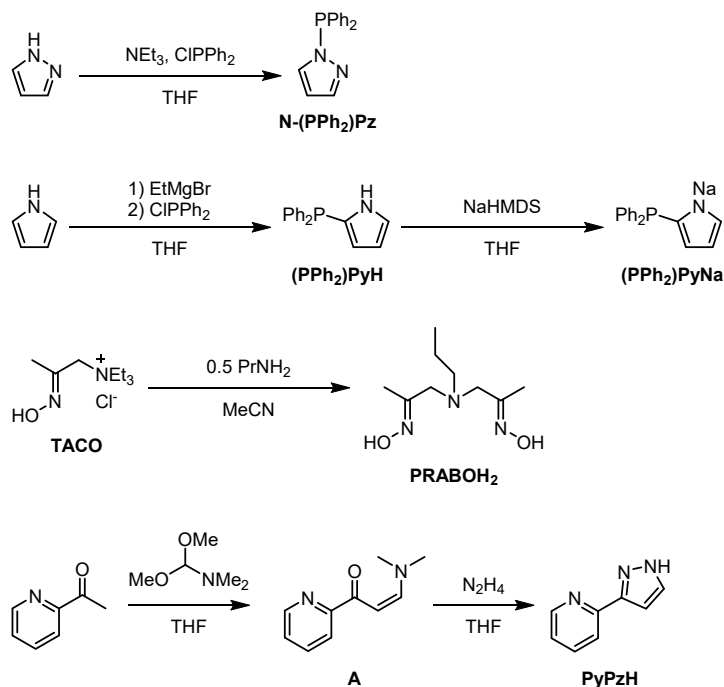
Many ligands were surveyed to determine which ligands would be most suitable to the stabilization of heterometallic [Fe₃M]-type complexes. With the aim of supporting low-valent apical Ni centers, **N-(PPh₂)Pz** and **(PPh₂)PyH** were synthesized according to literature protocols (Scheme 1).[5] The softer phosphine donors would be expected to preferentially bind the apical metal based on steric clash with the **LH₃** ligand to form a N-anchored three-atom bridge to the Fe₃ core. Conceptually, these ligands would replace bridging acetate ligands commonly observed in other multimetallic complexes reported by our group. The reaction of **(PPh₂)PzH** with sodium hexamethyldisilazide (NaHMDS) cleanly afforded the deprotonated pyrrole moiety, **(PPh₂)PzNa**. This opens up multiple avenues for ligand incorporation into clusters with both salt metathesis or protonlysis routes viable depending on ligand precursor utilized.

Multidentate chelating ligand architectures were also pursued to provide additional donors to support the apical metal center. To this end, **PRABOH₂** and **PyPzH** were also synthesized according to literature procedures (Scheme 1).[6] Unpublished results in the group had studied the use of these ligands in tetranuclear clusters suggesting their application to the synthesis of [Fe₃Ni] clusters would be worth pursuing.[7]

Section A.2 Attempts to Synthesize [Fe₃Ni(μ₄-S)] Clusters

To better mimic the active site of [NiFe] CODH, an interstitial sulfide was targeted. The addition of bis(trimethylsilyl)sulfide (S(SiMe₃)₂) to a cationic [Fe^{II}₃(OAc)₂(OTf)] (OTf = trifluoromethanesulfonate or triflate) complex (**2**) in acetonitrile (MeCN) cleanly afforded the desired Fe₃(μ₃-S) (**3**) cluster in quantitative yield by NMR with loss of trimethylsilylacetate. This represents a different synthetic strategy compared to other tetranuclear oxido-containing clusters reported from our group which require an oxidative installation of the interstitial atom. Compound **3** could also be cleanly be isolated from the corresponding [Fe^{II}₃(OAc)₃] complex (**1**) in a one-pot procedure in MeCN by first generating **2** *in situ* by adding half an equivalent of calcium triflate to act as an acetate sink. S(SiMe₃)₂ was then added resulting in an immediate color change to a red solution characteristic of **3**.

Scheme 2. Syntheses of Fe₃(μ₃-S) Cluster

d(Fe-S1)	d(Fe-O4)
Fe1: 2.3751(13)	Fe1: 2.098(2)
Fe2: 2.4033(13)	
Fe3: 2.4119(13)	

d(Fe-Fe)	d(Fe-Fe)
Fe1-Fe2: 2.977	Fe1-Fe1': 3.120
Fe1-Fe3: 2.927	
Fe2-Fe3: 2.955	
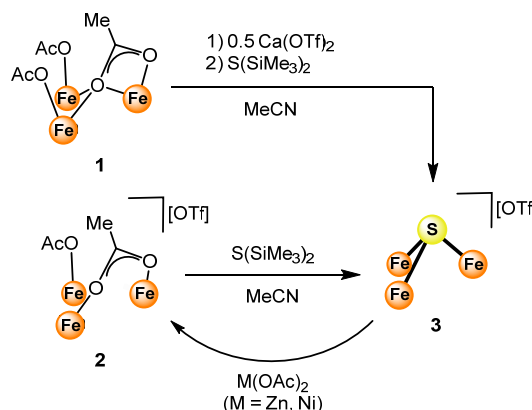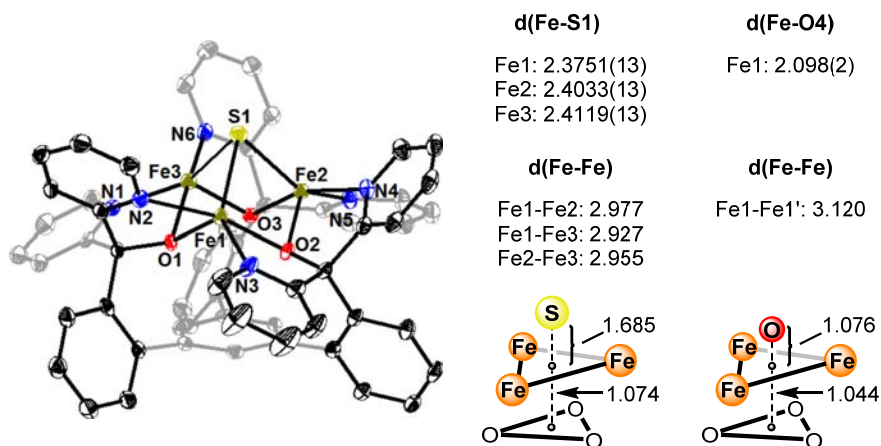
Figure 4. Solid-state structure of complex **3**. Hydrogen atoms, solvent molecules, and counterions have been omitted for clarity. Select bond metrics for **3** and the cationic $[Fe^{II}_3(\mu_3\text{-O})(MeCN)_3]$ cluster are also presented.

The $[Fe^{II}_3(\mu_3\text{-S})]$ assignment was confirmed by single crystal X-ray diffraction (XRD) analysis with samples recrystallized from acetonitrile/ether vapor diffusion (Figure 4). In the solid-state, each Fe center is five-coordinate and shows distorted square pyramidal geometry with an intermediate τ_5 parameter for each Fe center (Fe1: 0.43, Fe2: 0.34, Fe3: 0.31). This differs substantially from a crystallographically characterized $[Fe^{II}_3(\mu_3\text{-O})]$ complex with the same metal oxidation states. The smaller oxide interstitial atom enables where acetonitrile coordination to each Fe center, resulting in 6-coordinate *pseudo*-octahedral metal centers. Consistent with the larger size of the interstitial sulfur atom relative to the oxygen Fe–X distances are considerably elongated in compound **3**, ranging from 2.3751(13) to 2.4119(13) Å, compared to 2.098(2) Å in the case of the $[Fe^{II}_3(\mu_3\text{-O})]$ complex. As a consequence, the distances between the Fe₃-centroid and the interstitial atom elongates from 1.076 to 1.685 Å representing a substantial 0.61 Å shift. The sum of the angles around the interstitial atom are also markedly different shrinking with the larger sulfur atom to 228.18 ° versus

288.19 ° in the case of the (μ_3-O) ligand. Counterintuitively, the Fe–Fe distances contract for compound **3** (2.977, 2.927, 2.955 Å) relative to the [Fe$^{II}_3$(μ_3-O)] complex (3.120 Å), which necessarily results in a elongation of the Fe$_3$ centroid to (alkoxide-O)$_3$ centroid distance from 1.044 to 1.074 Å.
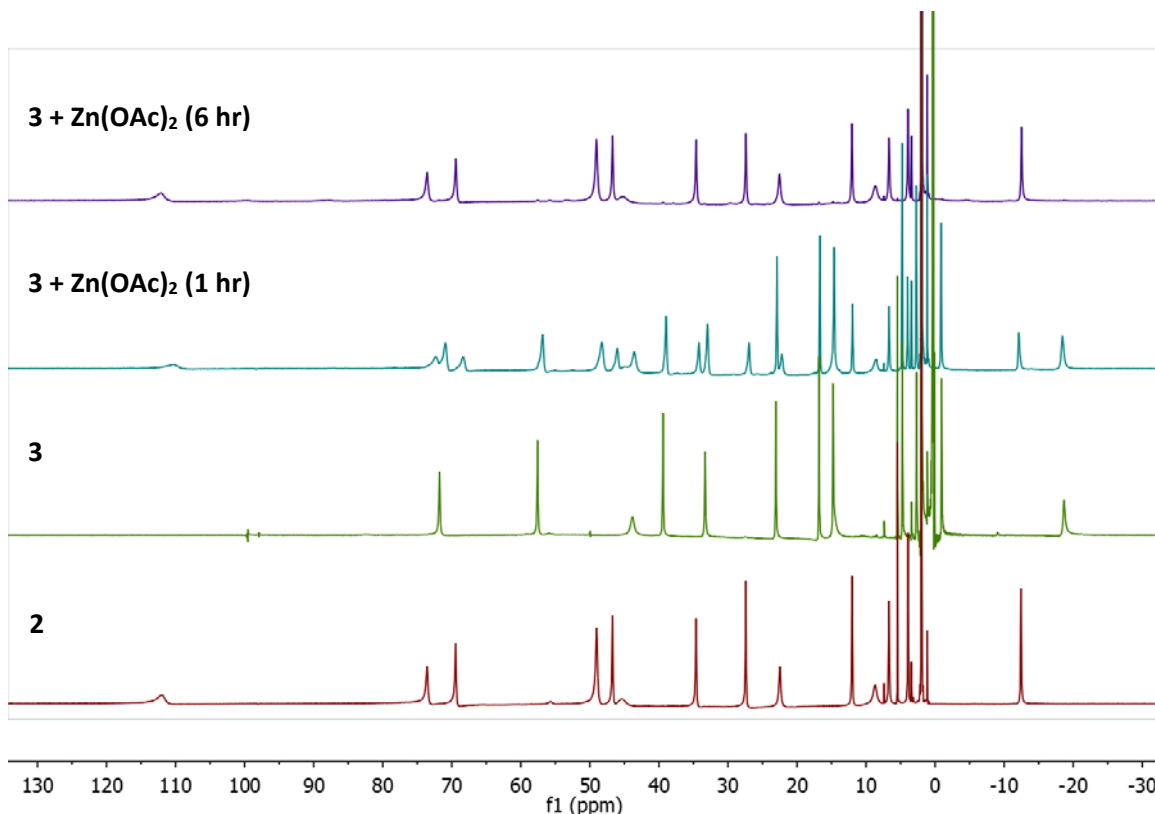
Figure 5. ^{1}H NMR data showing the quantitative conversion of **3** into **2** following addition of Zn(OAc)$_2$.

Despite the convenient ability to isolate compound **3**, the installation of the fourth metal center proved challenging. Previously reported tetranuclear clusters have always required supporting ligands such as acetates or pyrazolates. Therefore the binding to **N-(PPh₂)Pz** and **(PPh₂)PyNa** to compounds **3** was pursued. However, these reactions only resulted in a complicated mixture of products by NMR that could not be purified or characterized. The addition of Ni^{II}- or Zn^{II}(OAc)$_2$ salts also resulted in

the conversion of **3** back into the bis(acetate) complex **2** over multiple hours (Figure 5). A dark precipitate also formed consistent with loss of insoluble metal chalcogenides byproducts. Attempts to oxidize compound **3** with ferrocenium salts also resulted in complicated mixtures by NMR from which Fe_3Cl_n complexes could be crystallized indicating loss of the interstitial sulfide. As a result it became apparent that the installation of the fourth metal center using **3** was difficult due to the propensity to lose the sulfide either as metal chalogenides or as elemental sulfur. Efforts to construct [NiFe] CODH model complexes turned to alternative strategies.

Section A.3 Attempts to Synthesize [Fe₃Ni(μ₄-O)] Clusters

After attempts to construct higher nuclearity clusters with compound **3** proved unsuccessful, efforts turned to the synthesis [Fe₃Ni] clusters with a (μ₄-O) ligand to build off of established results in the group with asymmetric [Fe₃M(μ₄-O)]-type clusters.[7] Previous results in the group suggested that [Fe₄O] and [Fe₃ZnO] clusters had been accessible using **PyPzH** or **PRABOH₂** in conjunction with acetate ligands.[7] Therefore, the use of these ligands when constructing [Fe₃Ni] clusters was pursued. Due to the low propensity of Ni^{II} to coordinate carbon dioxide efforts focused on the isolation of [Fe₃Ni] possessing a bridging or terminal hydroxide ligand whose nucleophilic attack on carbon monoxide or isoelectronic analogs could be studied.

Initial efforts focused on transmetalation reactions from a previously reported [Fe₃Ca(μ₄-O)(μ₂-OH)] complex (**4**) which had served as the precursor to a variety of heterometallic [Fe₃M]-type clusters. The addition of Ni(OTf)₂ was found to result in the quantitative recovery of starting material. As numerous other M(OTf)ₙ salts have previously been shown to transmetallate in [Mn₃CaO₄] and [M₃Ca(μ₄-O)(μ₂-OH)] (M = Mn, Fe) clusters,[4c, 4d, 8] it was proposed that the low solubility of the nickel precursor led

to the lack of observed reactivity. To improve the solubility of the nickel precursor, transmetalation reactions with $Ni(MeCN)_6(OTf)_2$ were attempted, however again no conversion was observed (Scheme 3). A clean reaction to form a new species was observed if $NiCl_2(dme)$ was used as the nickel source. However, a solid-state structure obtained of the product indicated the formation of a cationic $[Fe^{III}_3Cl_3(\mu_3\text{-}O)]$ cluster (**5**) indicating loss of the calcium center without nickel incorporation. A structurally related $[Fe^{II}_3Cl_3]$ complex (**6**) without the bridging oxido ligand could be accessed directly from **LH$_3$** by adapting the synthetic protocols for **1** to utilize $FeCl_2$ rather than $Fe(OAc)_2$ as the iron precursor. Of note a more efficient synthesis has been recently developed by Charlie Arnett in the group, which involves the addition of trimethylsilylchloride to **1**. This protocol avoids the difficult to remove triethylammonium derived salts and should be used and the synthesis for complex **6** in the future. A preliminary solid-state structure with highly disordered solvent was obtained for **6** allowing direct comparison to complex **5** (Figure 6).

Scheme 3. Synthesis of Fe$_3$Cl$_3$–type compounds

d(Fe-O4)

Fe1: 1.9222(13)
Fe2: 1.9457(13)
Fe3: 1.9107(14)

d(Fe-Fe)

Fe1-Fe2: 3.021
Fe1-Fe3: 3.015
Fe2-Fe3: 3.025

d(Fe-Fe)

Fe1-Fe2: 3.291
Fe1-Fe3: 3.309
Fe2-Fe3: 3.368
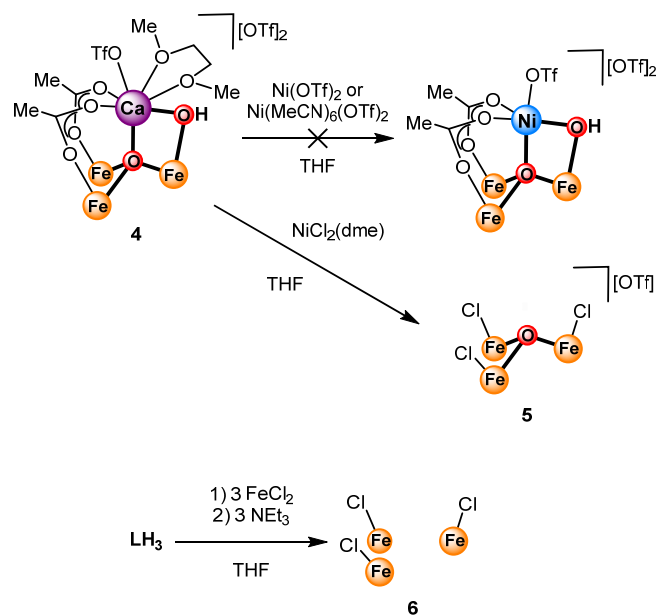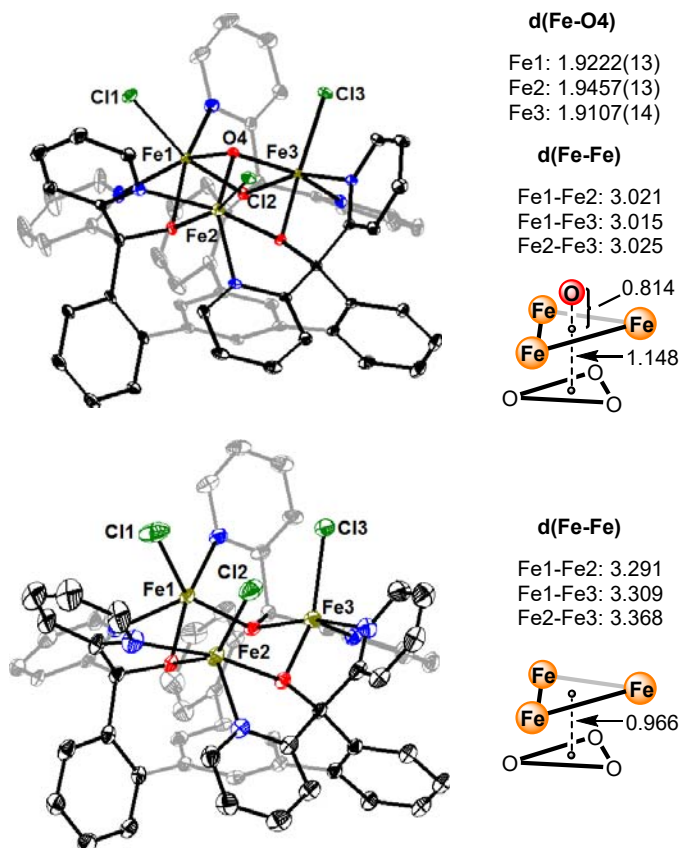
Figure 6. Solid-state structures of **5** (top) and **6** (bottom). Hydrogen atoms, solvent molecules, and counterions have been omitted for clarity.

The (μ_3-O) ligand of **5** helps enforce shorter average Fe–Fe distances (3.02 Å) compared to **6** (3.32 Å) by approximately 0.3 Å. As a result the Fe_3 centroid to (alkoxide-O)$_3$ centroid distance is longer in **5** compared to **6**, 1.148 and 0.966 Å respectively, due to the geometric constraints of the chair cyclohexane-like core of the complex. Complex **6** shows distorted square planar geometries around each Fe center with τ_5 parameters of 0.393, 0.436, and 0.330 for Fe1, Fe2, and Fe3 respectively. The metrics of **5** can also be compared to the cationic [$Fe^{II}_3(MeCN)_3(\mu_3$-O)]. Consistent with higher oxidation state of each Fe center (Fe^{III} vs Fe^{II}) in complex **5**, shorter Fe-O4 (d(Å): Fe1: 1.9222(13), Fe2: 1.9457(13), Fe3: 1.9107(14)), Fe-Fe (d(Å): Fe1-Fe2: 3.021,

Fe1-Fe3: 3.015, Fe2-Fe3: 3.025), and Fe$_3$ centroid to (alkoxide-O)$_3$ centroid distances (0.814 Å) are observed.

As transmetalation reactions directly from **4** proved unsuccessful, efforts to substitute supporting ligands prior to transmetalation was attempted. Previous results had shown that **PRABOH$_2$** substitution onto **4** resulted in selective protonlysis with the (μ$_2$-OH) resulted in the formation of complex **7** (Scheme 4). From complex **7** the addition of Ni(MeCN)$_6$(OTf)$_2$ was found to cleanly yield a new species by NMR (**8**).

Scheme 4. Synthesis and reactions of **PRABOH$_2$** stabilized Fe$_3$Ni complexes
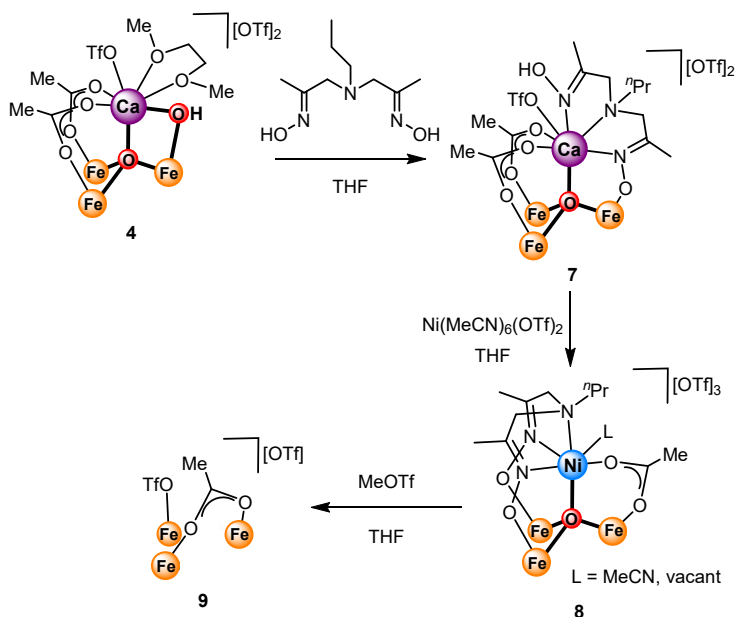
Two solid-state structures for **8** was obtained, which confirmed the formation of a dicationic [Fe$_3$Ni] complex with a formal oxidation state assignment of [Fe$^{III}_2$Fe^{II}Ni^{II}] indicating cluster reduction from the Fe$^{III}_3$ oxidation state of **7** has occurred. Transmetalation of calcium for nickel results the **PRABOH$_2$** substitution for another acetate resulting in both oximate oxygens coordinating to Fe2 and Fe3, which is likely attributable to the small size of nickel compared to calcium. The remaining three nitrogeneous donors of the **PRABOH$_2$** ligand form a facially coordinating chelate for

the apical Ni center. Different geometries around the apical Ni center are observed in the different solid-state structures with one showing a 5-coordinate *pseudo*-square planar geometry ($\tau_5 = 0.44$) while acetonitrile coordination in the second structure results in a *pseudo*-octahedral nickel geometry. While the *pseudo*-octahedral structure is of low-quality (R1 = 16.3%), the crystal structure of the 5-coordinate nickel was of sufficient quality to thoroughly analyze the bonding metrics. Elongation of the Fe1–O4 distance (2.079(3) Å) relative to the comparable distances for Fe2 and Fe3, 1.942(3) and 1.960(3) Å respectively, is indicative of localization of the Fe^{II} center in the Fe1 position. The Ni1–O4 distance is slightly shorter than the Fe–O4 distances at 1.924(3) Å. Complex **8** shows O4 to Fe$_3$ centroid (0.929 Å) and Fe$_3$ centroid to (alkoxide-O)$_3$ centroid (1.096 Å) distances that are intermediate to **5** and the [Fe$_3$(MeCN)$_3$(μ_3-O)] centroid, however structural and oxidation state differences preclude further interpretation of these comparisons.

Efforts to open up a bimetallic edge site by acetate removal were then pursued. As trimethylsilyl triflate had previously been shown to oxidize clusters, the addition of methyl triflate to **8** was attempted. NMR reactions indicated the formation of a previously reported [Fe$_3$(OAc)(OTf)$_2$] complex (**9**) suggesting loss of the apical nickel center along with the **PRABOH$_2$** ligand had also occurred. Consequently, further efforts to install hydroxide ligands or bind carbon dioxide to complex **8** were discontinued.

Similar attempts to construct [Fe$_3$Ni] clusters with a previously synthesized Fe$_3$ mono(**PyPz**) bis(acetate) precursor (**7**). The addition of Ni(MeCN)$_6$(OTf)$_2$ to complex **10** did not result in the formation of a [Fe$_3$Ni] complex, but rather the loss of the PyPz ligand from the triiron core. Low quality crystals identified an iron-containing product

as a different structural form of the $[Fe_3(OAc)(OTf)_2]$ complex (**11**). If iodosylbenzene (PhIO) was added prior to $Ni(MeCN)_6(OTf)_2$ a complicated mixture of species was formed by NMR, however low quality crystals confirmed the formation of a $[Fe_3Ni]$ species. Unfortunately, efforts to reproduce these results of purify reactions products proved unsuccessful and this approach to [NiFe] heterobimetallic clusters was also discontinued.

d(M-O4)

Fe1: 2.079(3)
Fe2: 1.942(3)
Fe3: 1.960(3)
Ni1: 1.924(3)

d(Fe-Fe)

Fe1-Fe2: 3.075
Fe1-Fe3: 3.009
Fe2-Fe3: 3.087

d(X-Ni)

N7: 1.956(5)
N8: 1.985(5)
N9: 2.091(5)
O6: 1.945(4)
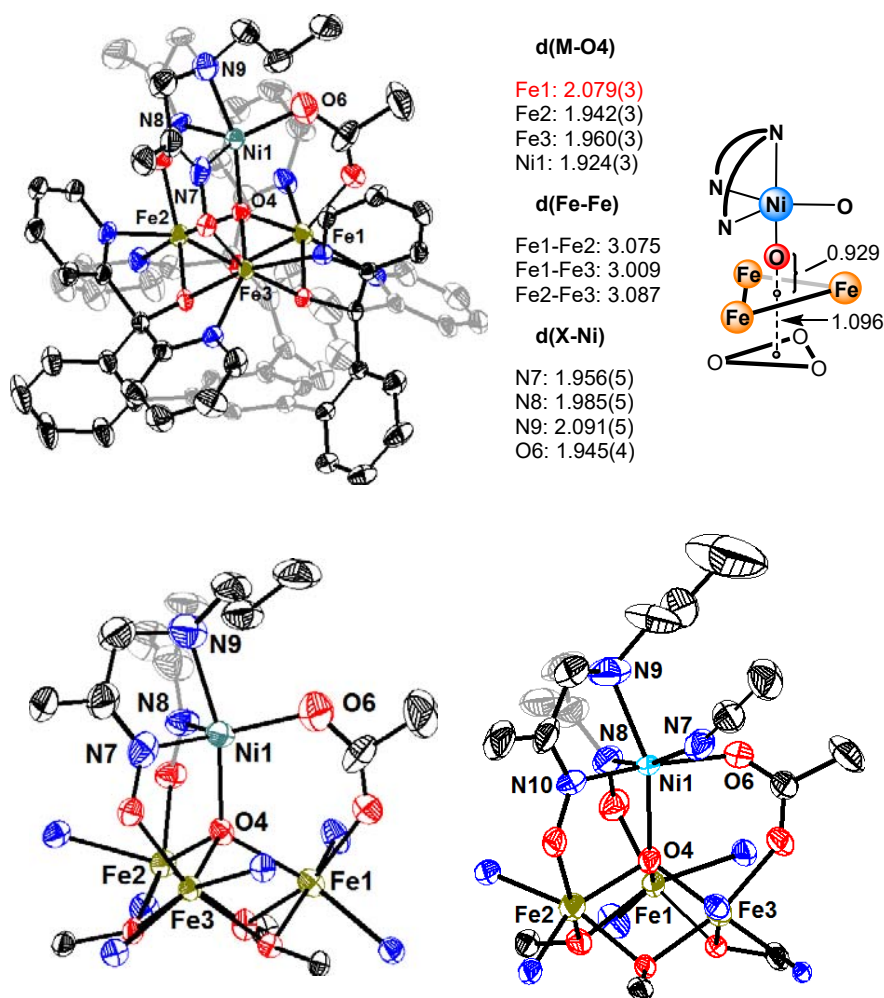
Figure 7. Solid-state structures of **8** with and without acetonitrile coordination. Hydrogen atoms, solvent molecules, and counterions have been omitted for clarity.

Scheme 5. Attempted synthesis of [Fe₃Ni] complexes
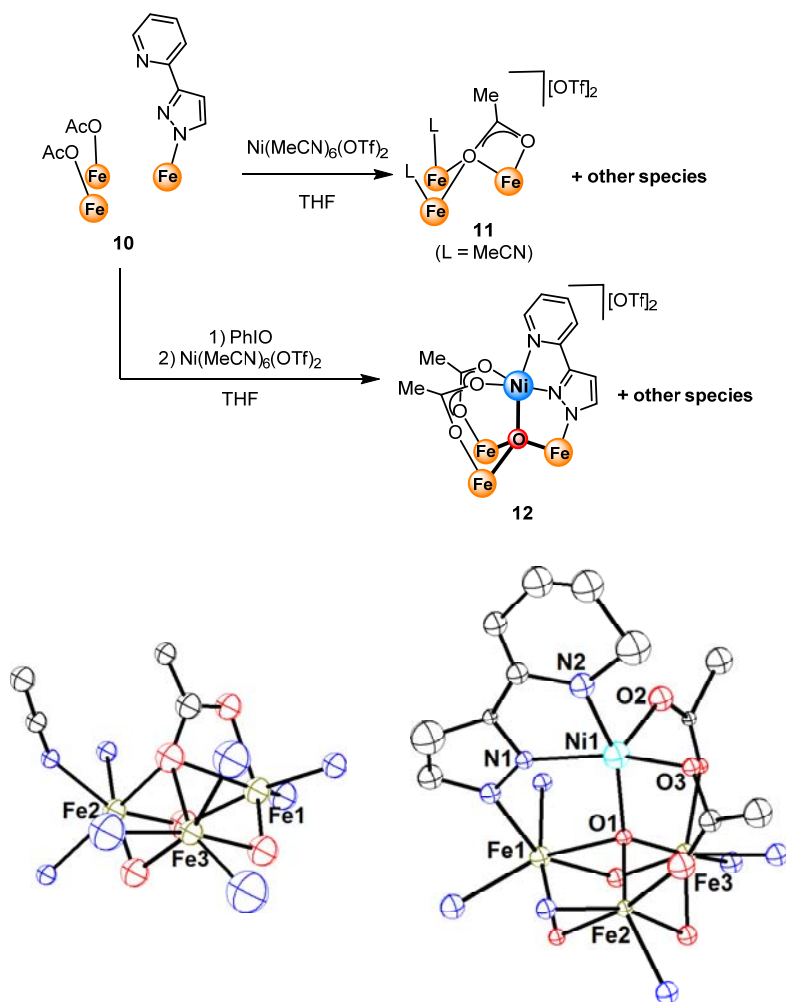
Figure 8. Preliminary solid-state structures for **11** and **12**.

CONCLUSIONS

Multiple attempts to rationally synthesize and study [Fe₃Ni] complexes as CODH active site models proved unsuccessful. However, several key caveats to design of tetranuclear clusters for subsequent projects could be gleaned from these studies. The first is the difficulty with utilizing the heavier main group elements as the interstitial atoms in higher nuclearity clusters. The substantial elongation of Fe–X bonds seen between compound **3** and the $[Fe^{II}_3(MeCN)_3(\mu_3\text{-O})]$ cluster (~0.3 Å)and the increase in the Fe₃ centroid to X distance (~0.6 Å) result in *pseudo*-square pyramidal 5-coordinate

Fe centers which are reluctant to coordinate sixth ligands. The loss of metal chalcogenide salts during attempts to construct tetranuclear clusters also proved problematic. Furthermore, the softer nature of the sulfide donor made oxidations while retaining the (μ_3-S) moiety infeasible as the formation of chloride species was observed in these reactions, likely arising from reaction with dichloromethane as the solvent. In combination, the inability to easily bind exogenous ligands, incorporate fourth metal centers, or oxidize the cluster resulted in a complex that, while structurally different from previously reported complexes in our group, was not compatible with the targeted biomimetic complexes.

The second design principle is the strengths and limitations of the utilizing stabilizing chelating architectures to access tetranuclear clusters. The use of **PRABOH₂** allowed for the isolation of [Fe₃Ni] clusters which was not possible with acetate ligands present in **4** demonstrating the type of donors available to the apical metal during transmetalation reactions also plays a role. However, this tight chelation of the apical metal can also result in synthetic complications when attempting to remove ligands with exogeneous electrophiles such as methyl triflate. While in principle the chelating nature of **PRABOH₂** was intended to promote removal of the remaining acetate ligand, loss of the chelating ligand and apical metal together proved to be the favorable reaction. The use of exogeneous metal salts to remove cluster-bound ligands has been previously been demonstrated in the synthesis of compound **2**, which is conveniently synthesized from compound **1** in MeCN with half an equivalent of calcium triflate. This was also implicated in reactions of **10** with Ni(MeCN)$_6$(OTf)$_2$ as crystals of **11** were obtained indicating removal of the **PyPz** ligand by the nickel center under reaction conditions. Taken together these data suggest a balance between chelating to the apical metal and

binding strength to the Fe$_3$ core exists to maintain a stable tetranuclear cluster. Though recent success with three-fold symmetric pyrazolate [Fe$_4$O]-type clusters has allowed for the stabilization of a vacant coordination site on the apical metal center, access to reactive dinuclear edge sites continues to be a challenge to due to asymmetry and reduced stability of these synthetic targets.

EXPERIMENTAL SECTION

General considerations.

All air- and/or water-sensitive compounds were manipulated using standard vacuum or Schlenk line techniques or in an inert atmosphere glove box. The solvents for air- and moisture-sensitive reactions were dried over sodium benzophenone ketyl, calcium hydride, or by the method of Grubbs.[9] All NMR solvents were purchased from Cambridge Isotopes Laboratories, Inc. and dried over sodium benzophenone ketyl or calcium hydride. Unless mentioned otherwise, reagents were used as received from commercial suppliers without further purification. **1**,[10] **2**,[7] **4**,[8a] **10**,[7] **N-(PPh₂)Pz**,[5b] **(PPh₂)PyH**,[5a] **PRABOH₂**,[6a] and **PyPzH**[6b] were synthesized according to reported procedures. Methyl triflate, bis(trimethylsilyl)sulfide, iodobenzene diacetate, and triethylamine was purchased from Sigma Aldrich, dried over calcium hydride, and then distilled prior to use. Calcium triflate, zinc acetate, nickel triflate, nickel acetate, nickel dichloride dimethoxyethane adduct, iron chloride were purchase from Strem Chemicals Inc. All ^{1}H, ^{13}C, and ^{31}P spectra were recorded on Varian Mercury 300 MHz, or Varian INOVA-500 or 600 MHz spectrometers at room temperature. Chemical shifts for ^{1}H and ^{13}C NMR data are reported relative to residual solvent peaks.[11] ^{31}P NMR chemical shifts are reported with respect to the deuterated solvent used to lock the instrument. Elemental analyses were performed by Robertson Microlit Laboratories, Ledgewood, NJ.

Synthesis of Complex 3 from 2

2 (196 mg, 0.151 mmol, 1 equiv) was partially dissolved in acetonitrile (20 mL) and then transferred to a Schlenk tube fitted with a screw-in Teflon stopper. While stirring bis(trimethylsilyl)sulfide (50 μL, 0.237 mmol, 1.56 equiv) was added as a acetonitrile solution

(1 mL). The reaction was then allowed to stir for 16 hours during which time the solution changed color from bright yellow to a deep red. The reaction mixture was then pumped down to yield a dark red solid. This residue was then suspended in minimal acetonitrile as filtered onto a Celite pad. The remaining red solid was brought through the Celite pad with dichloromethane. The dichloromethane filtrate was then dried under reduced pressure. The crude product was the purified by recrystallization from the vapor diffusion of diethyl ether into a concentrated dichloromethane solution. The pure product was obtained a dark red crystals and a red powder. Yield: 90 mg (49 %).

Synthesis of Complex 3 from 1

1 (299 mg, 0.249 mmol, 1 equiv) was suspended in acetonitrile (20 mL) and transferred to a Schlenk tube fitted with a screw-in Teflon stopper. Calcium triflate (42.1 mg, 0.124 mmol, 0.5 equiv) was then added as a solution in acetonitrile, which resulted in a gradual color change from a pale orange suspension to a homogeneous bright yellow color characteristic of [LFe$_3$(OAc)$_2$][OTf] after 30 minutes. Bis(trimethylsilyl)sulfide (66.7 μL, 0.374 mmol, 1.5 equiv) was then added as a solution in acetonitrile. The reaction was then allowed to stir for 16 hours during which time a color change from bright yellow to a deep red was observed. The reaction mixture was then dried under reduced pressure to yield a red residue. The residue was then suspended in tetrahydrofuran and filtered onto a Celite pad. The red solid was then washed with additional tetrahydrofuran until washed became colorless before the product was brought through with dichloromethane. The combined dichloromethane filtrate was the dried under reduced pressure to yield the pure product without further purification as a red powder. Yield: 261 mg (87 %). ^{1}H NMR (300 MHz, CD$_3$CN) δ(ppm) 71.8, 57.5, 43.8, 39.3, 33.4, 23.0, 16.8,

14.7, 14.4, -0.98, -18.76. ^{19}F NMR (282 MHz, CD$_3$CN) δ(ppm) -79.2. Anal. Calcd. for: C$_{58}$H$_{39}$F$_3$Fe$_3$N$_6$O$_6$S$_2$ (**3**) (%): C, 57.83; H, 3.26; N, 6.98. Anal. Calcd. for: C$_{59}$H$_{41}$Cl$_2$F$_3$Fe$_3$N$_6$O$_6$S$_2$ (**3**•(CH$_2$Cl$_2$)) (%): C, 54.95; H, 3.20; N, 6.52. Found: C, 55.10; H, 3.16; N, 6.74.

Synthesis of Complex 5

Complex **4** (359 mg, 0.204 mmol, 1 equiv) was dissolved in acetonitrile (15 mL). This solution was then transferred to a 20 mL scintillation vial containing nickel dichloride dimethoxyethane adduct (67.5 mg, 0.303 mmol, 1.5 equiv). The reaction mixture was then allowed to stir for 16 hours during which time the NiCl$_2$(dme) became homogeneous. The reaction mixture was dried under reduced pressure to yield an orange residue. The residue was suspended in tetrahydrofuran and filtered onto a Celite pad. The orange solid was then washed with tetrahydrofuran until the washes became colorless. The product was then brought through with dichloromethane. The combined dichloromethane filtrate was then dried under reduced pressure to yield the pure product without further purification as an orange powder. Yield: 164 mg (61.8 %).^{1}H NMR (300 MHz, CD$_3$CN) δ(ppm) 126.9, 97.3, 61.5, 59.3, 58.3, 53.2, 14.7, 13.5, 8.7, 6.8. ^{19}F NMR (282 MHz, CD$_3$CN) δ(ppm) -78.9. Anal. Calcd. for: C$_{58}$H$_{39}$Cl$_3$F$_3$Fe$_3$N$_6$O$_7$S$_2$ (**5**) (%): C, 53.80; H, 3.04; N, 6.49. Anal. Calcd. for: C$_{59}$H$_{41}$Cl$_5$F$_3$Fe$_3$N$_6$O$_7$S$_2$ (**5**•(CH$_2$Cl$_2$)) (%): C, 51.36; H, 3.00; N, 6.09. Found: C, 51.27; H, 3.00; N, 5.82.

Synthesis of Complex 6

LH_3 (303.4 mg, 0.353 mmol, 1 equiv.) and $FeCl_2$ (134.3 mg, 1.059 mmol, 3 equiv.) was transferred into a Schlenk tube fitted with a screw-in Teflon stopper and equipped with a magnetic stirbar. Dichloromethane (*ca.* 40 mL) was then added. Triethylamine (152.8 μL, 1.09 mmol, 3.1 equiv.) was then added and the reaction vessel sealed and allowed to stir for 16 hrs at room temperature. Reaction volatiles were then removed under reduced pressure. The residue was then triturated with tetrahydrofuran and the solids collected on a Celite pad. The product was then eluted with copious dichloromethane. The filtrate volatiles were then removed under reduced pressure. Following purification with tetrahydrofuran washes, the product becomes largely insoluble and difficult to work with. Complete removal of triethylammonium salts proved difficult proved challenging and the low solubility of the product in dichloromethane precluded recrystallization on substantial scales. An improved synthesis, which should be used for all future preparations, has been developed by Charlie Arnett in the Agapie group. ^{1}H NMR (300 MHz, CD_2Cl_2) δ 108.90, 76.86, 73.32), 61.31, 51.72, 42.25, 26.22, 15.86, 12.84, 9.96, 8.73, 8.10, -7.56.

Synthesis of Complex 8

Compound **4** (102.8 mg, 0.059 mmol, 1 equiv.) was transferred to a 20 mL scintillation vial equipped with a magnetic stirbar. **PRABOH₂** (11.8 mg,0.059 mmol, 1 equiv.) was then added as a tetrahydrofuran solution (*ca.* 4 mL) and the reaction mixture was allowed to stir for 6 hrs at room temperature to ensure formation of **7**. $Ni(MeCN)_6(OTf)_2$ (35.4 mg, 0.059 mmol, 1 equiv.) was then added as a solution in THF (*ca.* 4 mL) and the combined reaction mixture

allowed to stir for 16 hrs at room temperature. The reaction volatiles were then removed under reduced pressure. The residue was then triturated with dichloromethane a filtered through a Celite pad to remove salts from the product. The DCM filtrates were then dried under reduced pressure and the product obtained as a brown solid. Yield: 77 mg (80 % calculated if no MeCN coordinated to Ni center). ^{1}H NMR (300 MHz, CD$_3$CN) δ 185.37, 184.47, 164.06, 94.29, 92.43, 90.76, 86.93, 84.69, 83.16, 81.44, 78.88, 78.28, 76.66, 74.83, 48.61, 45.90, 37.37, 17.36, 16.66, 12.08, 9.33, 8.49, -0.53, -1.91, -4.73, -18.95, -27.69. ^{19}F NMR (282 MHz, CD$_3$CN) δ -79.08.

Crystallographic Information

Refinement Details

In each case, crystals were mounted on a glass fiber or nylon loop using Paratone oil, then placed on the diffractometer under a nitrogen stream. Low temperature (100 K) X-ray data were obtained on a Bruker APEXII CCD based diffractometer (Mo sealed X-ray tube, K_α = 0.71073 Å). All diffractometer manipulations, including data collection, integration and scaling were carried out using the Bruker APEXII software.[12] Absorption corrections were applied using SADABS.[13] Space groups were determined on the basis of systematic absences and intensity statistics and the structures were solved by direct methods using XS (incorporated into SHELXTL) and refined by full-matrix least squares on F^2. All non-hydrogen atoms were refined using anisotropic displacement parameters. Hydrogen atoms were placed in idealized positions and refined using a riding model. The structure was refined (weighted least squares refinement on F^2) to convergence.

Table 1. Crystal and refinement data for complexes reported in Appendix A

Complex	3	5	6	8	8 (MeCN-bound)
empirical formula	$C_{66}H_{55}F_3Fe_3N_8O_7S_2$	$C_{62}H_{42}Cl_3F_3Fe_3N_8O_7S$	$C_{57}H_{39}Cl_3Fe_3N_6O_3$	$C_{78}H_{59}F_6Fe_3N_9Ni_{0.94}O_{16}S_2$	$C_{136}H_{0.50}F_{12}Fe_6Ni_2O_{26}S_4$
formula wt	1360.85	1373.99	1129.84	1779.20	3138.82
T (K)	100	100	100	100.01	99.99
a, Å	12.5685(13)	11.5004(4)	14.1495(8)	19.3212(6)	15.9295(7)
b, Å	32.915(4)	14.8380(5)	16.7479(9)	16.7299(5)	22.5961(10)
c, Å	14.5295(15)	18.0383(6)	27.1921(14)	25.9311(8)	26.0003(11)
α, deg	90	97.2724(11)	90	90	101.7460(10)
β, deg	98.698(3)	106.1004(11)	94.550(2)	111.6010(10)	102.1610(10)
γ, deg	90	91.9710(12)	90	90	97.1460(10)
V, Å³	5941.5(11)	2925.77(17)	6423.5(6)	7793.3	8819.2(7)
Z	4	4	4	4	2
cryst syst	Monoclinic	Triclinic	Monoclinic	Monoclinic	Triclinic
space group	P1 2₁/c 1	P-1	P 1 2_c 1	P 1 2₁/c 1	P-1
d_{calcd}, g/cm³	1.521	1.928	1.485	1.516	1.182
θ range, deg	1.547 to 28.513	2.374 to 36.523	2.165 to 30.536	2.275 to 30.509	2.429 to 30.154
μ, mm⁻¹	0.866	1.292	1.014	0.912	0.808
abs cor	Semi-empirical from equivalents	Semi-empirical from equivalents	Semi-empirical from equivalents	Semi-empirical from equivalents	Semi-empirical from equivalents
GOF[c]	1.038	1.921	2.987	1.019	1.377
R1,[a] wR2[b] (I > 2σ(I))	0.0721, 0.1729	0.0826, 0.2622	0.1300, 0.4038	0.0762, 0.1699	0.1631, 0.4159

[a] $R1 = \Sigma ||F_o|-|F_c|| / \Sigma|F_o|$ [b] $wR2 = \{ \Sigma [w(F_o^2-F_c^2)^2] / \Sigma [w(F_o^2)^2] \}^{1/2}$ [c] $GOF = S = \{ \Sigma [w(F_o^2-F_c^2)^2] / (n-p) \}^{1/2}$

REFERENCES

1.(a) Jones, J.-P.; Prakash, G. K. S.; Olah, G. A., *Israel Journal of Chemistry* **2014,** *54*, 1451-1466; (b) Qiao, J.; Liu, Y.; Hong, F.; Zhang, J., *Chemical Society Reviews* **2014,** *43*, 631-675; (c) Ren, D.; Deng, Y.; Handoko, A. D.; Chen, C. S.; Malkhandi, S.; Yeo, B. S., *ACS Catalysis* **2015,** *5*, 2814-2821.

2.(a) Can, M.; Armstrong, F. A.; Ragsdale, S. W., *Chemical Reviews* **2014,** *114*, 4149-4174; (b) Jeoung, J.-H.; Dobbek, H., *Science* **2007,** *318*, 1461-1464; (c) Jeoung, J.-H.; Dobbek, H., *Journal of the American Chemical Society* **2009,** *131*, 9922-9923.

3.(a) Ciurli, S.; Ross, P. K.; Scott, M. J.; Yu, S. B.; Holm, R. H., *Journal of the American Chemical Society* **1992,** *114*, 5415-5423; (b) Huang, D.; Holm, R. H., *Journal of the American Chemical Society* **2010,** *132*, 4693-4701; (c) Panda, R.; Zhang, Y.; McLauchlan, C. C.; Venkateswara Rao, P.; Tiago de Oliveira, F. A.; Münck, E.; Holm, R. H., *Journal of the American Chemical Society* **2004,** *126*, 6448-6459; (d) Yoo, C.; Kim, J.; Lee, Y., *Organometallics* **2013,** *32*, 7195-7203.

4.(a) de Ruiter, G.; Thompson, N. B.; Lionetti, D.; Agapie, T., *Journal of the American Chemical Society* **2015,** *137*, 14094-14106; (b) Kanady, J. S.; Tsui, E. Y.; Day, M. W.; Agapie, T., *Science* **2011,** *333*, 733-736; (c) Tsui, E. Y.; Agapie, T., *Proceedings of the National Academy of Sciences* **2013,** *110*, 10084-10088; (d) Tsui, E. Y.; Tran, R.; Yano, J.; Agapie, T., *Nat Chem* **2013,** *5*, 293-299.

5.(a) Dunn, P. L.; Reath, A. H.; Clouston, L. J.; Young Jr, V. G.; Tonks, I. A., *Polyhedron* **2014,** *84*, 111-119; (b) Yang, Y.; Liu, Z.; Liu, B.; Duchateau, R., *ACS Catalysis* **2013,** *3*, 2353-2361.

6.(a) Goldcamp, M. J.; Edison, S. E.; Squires, L. N.; Rosa, D. T.; Vowels, N. K.; Coker, N. L.; Krause Bauer, J. A.; Baldwin, M. J., *Inorganic Chemistry* **2003,** *42*, 717-728; (b) Yang, T.; Chen, G.; Sang, Z.; Liu, Y.; Yang, X.; Chang, Y.; Long, H.; Ang, W.; Tang, J.; Wang, Z.; Li, G.; Yang, S.; Zhang, J.; Wei, Y.; Luo, Y., *Journal of Medicinal Chemistry* **2015,** *58*, 6389-6409.

7.Thesis of Dr. Davide Lionetti, Appendix A

8.(a) Herbert, D. E.; Lionetti, D.; Rittle, J.; Agapie, T., *Journal of the American Chemical Society* **2013,** *135*, 19075-19078; (b) Suseno, S.; McCrory, C. C. L.; Tran, R.; Gul, S.; Yano, J.; Agapie, T., *Chemistry – A European Journal* **2015,** *21*, 13420-13430.

9.Pangborn, A. B.; Giardello, M. A.; Grubbs, R. H.; Rosen, R. K.; Timmers, F. J., *Organometallics* **1996,** *15*, 1518-1520.

10.Tsui, E. Y.; Kanady, J. S.; Day, M. W.; Agapie, T., *Chemical Communications* **2011,** *47*, 4189-4191.

11.Fulmer, G. R.; Miller, A. J. M.; Sherden, N. H.; Gottlieb, H. E.; Nudelman, A.; Stoltz, B. M.; Bercaw, J. E.; Goldberg, K. I., *Organometallics* **2010,** *29*, 2176-2179.

12.APEX2, Version 2 User Manual, M86-E01078, Bruker Analytical X-ray Systems, Madison, WI, June 2006.

13.Sheldrick, G. M. "SADABS (Version 2008/1): Program for Absorption Correction for Data from Area Detector Frames", University of Göttingen, 2008.